Supplementary Material (ESI) for Lab on a Chip

Supporting Information

Flow-focused synthesis of monodisperse gold nanoparticles using ionic liquids on a microfluidic platform

Laura L. Lazarus,[a] Astro S.-J. Yang,[b] Steven Chu,[b] Richard L. Brutchey*[a] and Noah Malmstadt*[b]

[a] Department of Chemistry, University of Southern California, Los Angeles, CA 90089, USA.
[b] Mork Family Department of Chemical Engineering and Materials Science, University of Southern California, Los Angeles, CA 90089, USA.

Materials and Methods.

Sodium borohydride (99%) and trichloro(1*H*,1*H*,2*H*,2*H*-perfluorooctyl)silane (97%), were purchased from Sigma-Aldrich (St. Louis, MO). 1-methylimidazole (99%) and 1-butyl-3-methylimadazolium tetrafluoroborate (98+%) were purchased from Alfa Aesar. Tetrachloroauric acid hydrate (99%) was purchased from Strem Chemicals (Newburyport, MA). All chemicals were used as received without further purification. The solutions were injected into the microfluidic device via syringe pump (Harvard Apparatus Pump 11 Plus) and monitored by a charge-coupled-device (CCD) camera (Canon Rebel Tli).

Powder X-Ray diffraction (XRD) patterns were acquired on a Rigaku Ultima IV X-ray diffractometer with a CuKα radiation source (λ = 1.54 Å). Transmission electron microscopy (TEM) and selected area electron diffraction (SAED) were performed on a JEOL JEM-2100 microscope at an operating voltage of 200 kV, equipped with a Gatan Orius CCD camera. Particle statistics were derived from populations of at least 300 nanoparticles. UV-vis absorption spectra were collected on a Shimadzu UV-1800 spectrophotometer in dual beam mode using quartz cuvettes with 1-cm path lengths from thiol stabilized gold nanoparticles dispersed in hexanes. Energy dispersive X-ray spectroscopic analysis was performed using a JEOL JSM-6610 scanning electron microscopy operating at 10 kV and equipped with an EDAX Apollo silicon drift detector.

Microfluidic Device Fabrication.

A positive SU-8(50) mold was fabricated through a standard photolithography process. Subsequently, a poly(dimethylsiloxane) (PDMS) stamp was cast onto the SU-8 mold and cured at 65 °C for 2 h. Following curing, the patterned surface was oxidized by a corona treater (BD-20AC, Electro-Technic Products, Chicago, IL) and directly bonded to a bare PDMS substrate. The bonded device was then heated at 65 °C for at least 2 h to recover PDMS surface hydrophobicity (Fig. S1). The microfluidic device was silanized with trichloro(1*H*,1*H*,2*H*,2*H*-perfluorooctyl)silane by deposition from the vapor phase for 20 min before each experiment.

Microfluidic Device Performance and Flow Behavior.

A fresh microfluidic device was fabricated for each nanoparticle synthesis run. Synthesis runs lasted as long as 4 h. No observable degradation in device performance was seen over the course of a run. AuNP deposition could be observed downstream of the reagent inlet junction in the form of a red-purple streak at the center of the channel. This

deposition was minimal and resulted neither in disruption of the flow pattern nor clogging of the channel.

Images of the two flow regimes are shown in Figure S2. Transition between these regimes occurred at an oil flow rate of about 3000 μL/h. The flow-focused streams were stable below an oil flow rate of 3000 μL/h, with no break-up into droplets occurring anywhere in the device. At higher flow rates, the droplet-forming streams demonstrated some instability, with the location of the droplet pinch-off point fluctuating over the course of an experiment. This point was generally located between the inlet junction and the first turn of the serpentine channel.

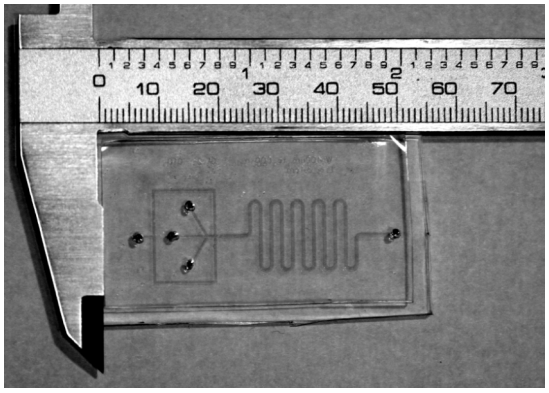

Fig. S1 Photographic example of the microfluidic chips used for this study.

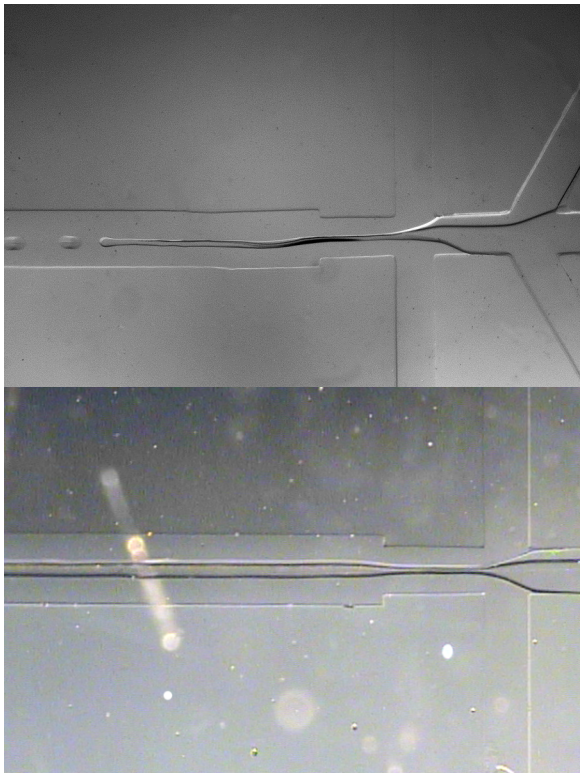

Fig. S2 Photographs of the two key microfluidic flow regimes. Top: droplet formation in the microfluidic channel with a 7000 μL/h flow rate of Halocarbon 6.3 oil. The ($HAuCl_4$ + 1-methylimidazole) and $NaBH_4$ reagent streams and pure BMIM-BF_4 streams were injected at flow rates of 90, 90, and 50 μL/h, respectively. Bottom: Focused flow without droplet break-up. All stream compositions and flow parameters are as described above, with the exception of the flow rate of the Halocarbon 6.3 stream, which here was 2070 μL/h.

TEM Micrographs and Other Data.

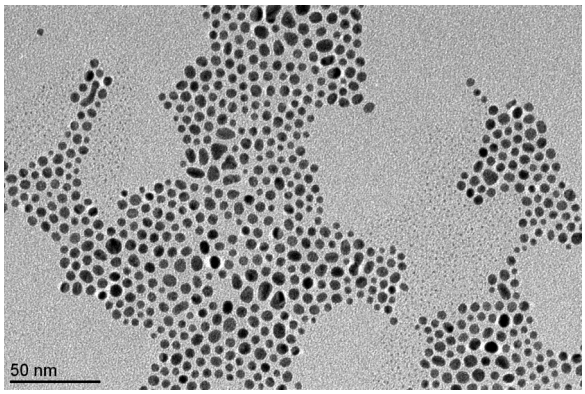

Fig. S3 TEM micrograph of AuNPs produced under flow focusing conditions. BMIM-BF_4 solutions of $NaBH_4$ and ($HAuCl_4$ + 1-methylimidazole), pure BMIM-BF_4, and Halocarbon 6.3 oil were injected at flow rates of 90, 90, 50, and 2070 μL/h, respectively.

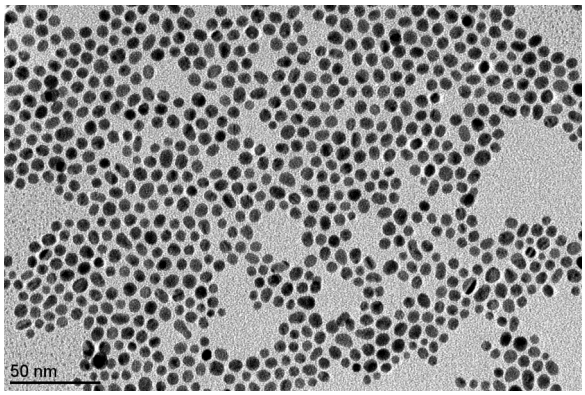

Fig. S4 TEM micrograph of AuNPs produced under laminar flow conditions. BMIM-BF_4 solutions of $NaBH_4$, ($HAuCl_4$ + 1-methylimidazole), and pure BMIM-BF_4 were injected at flow rates of 900, 900, and 500 μL/h, respectively.

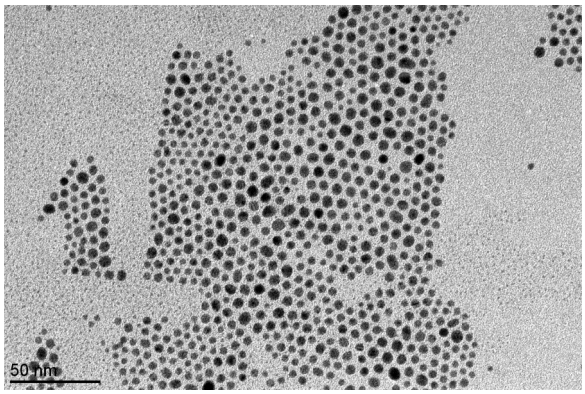

Fig. S5 TEM image of AuNPs produced in a general batch reaction. BMIM-BF_4 solutions of $HAuCl_4$, 1-methylimidazole, and $NaBH_4$ were combined in the presence of Halocarbon 6.3 oil (1:1:1:3 by vol., respectively).

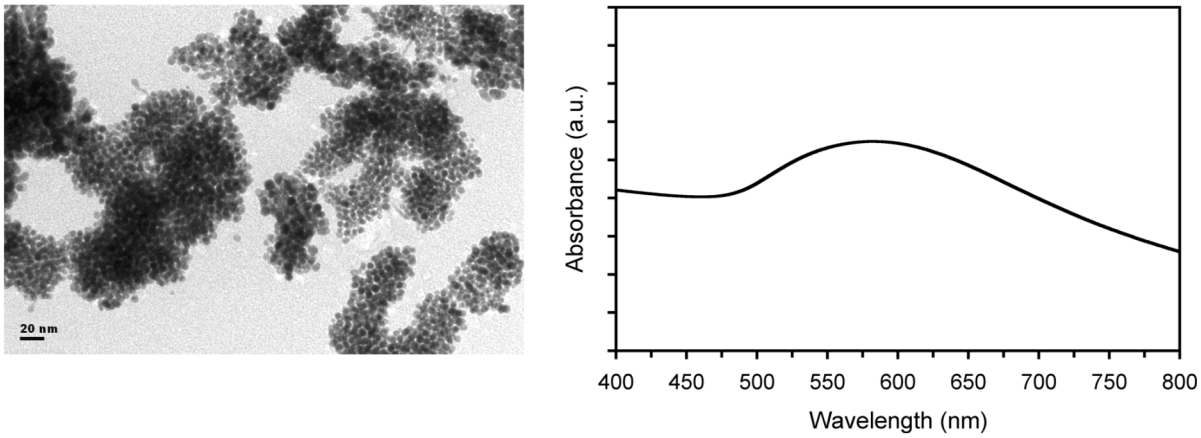

Fig. S6 (left) Representative TEM micrograph of agglomerated AuNPs prior to solvent transfer to hexanes and stabilization with 1-dodecanethiol. Characteristic of agglomerated AuNPs, the corresponding UV-vis spectrum (right) has a broader, red-shifted surface plasmon band (λ_{max} = 582.5 nm) compared to non-agglomerated AuNPs.

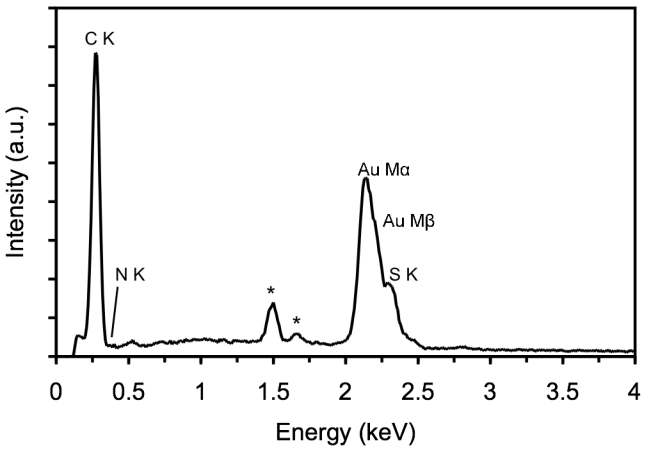

Fig. S7 Representative EDX spectrum of thiol-stabilized AuNPs. The asterisks indicate peaks originating from the substrate.